Research Article

BEARING FAULT DIAGNOSIS BASED ON CONVOLUTIONAL NEURAL NETWORK USING ESTIMATED MOTOR CURRENT SIGNALS AND THEIR SPECTRAL PORTRAIT

Huu Hai DANG[1], Ngoc-My BUI[2], Van-Phuc HOANG[3,] , Quy Thang BUI[3] , Van Sang DOAN[4]*

[1]Institute of Electronics, Academy of Military Science and Technology, Hanoi, Vietnam
[2]Department of Training, Academy of Military Science and Technology, Hanoi, Vietnam
[3]Institute of System Integration, Le Quy Don Technical University, Hanoi, Vietnam
[4]Vietnam Naval Academy, Khanhhoa, Vietnam

danghai1612@gmail.com, buingocmy_vn@mail.ru, phuchv@lqdtu.edu.vn, thangbq@lqdtu.edu.vn, doansang.g1@gmail.com

*Corresponding author: Van-Phuc Hoang; phuchv@lqdtu.edu.vn

Abstract. *Induction motor bearing fault diagnosis stands as a crucial aspect of rotating machinery maintenance. Numerous studies have delved into employing current signals and machine learning methods for this purpose. However, the effectiveness of these approaches relied heavily on manually selecting features for training. Moreover, traditional machine learning techniques struggle with large volumes of computational data. To address these limitations, researchers have turned to deep learning architectures such as Convolutional Neural Networks, ResNet, and AlexNet, either individually or in combination with traditional machine learning methods, for bearing fault diagnosis. Published convolutional neural network-based works usually use basic CNN networks. The experimental data are time or frequency domain data, and the fault classification accuracy is high only with noise-free signals. This paper proposes a novel approach aimed to enhance the accuracy of bearing fault identification by leveraging a CNN model trained on both the estimated motor current signals and their corresponding Fast Fourier Transform values. Comparative analysis against existing methodologies including machine learning and single-input convolutional neural networks or multi-input convolutional neural networks demonstrates that the proposed method achieves impressive results. The bearing fault accuracy reaches up to 99.88% for noise-free signals and 99.14% for signals with added noise at a Signal-to-Noise Ratio of -10 dB.*

Keywords

1. Introduction

In today's manufacturing sector, electric motors and all kinds of rotating electric devices are of significant importance. Consequently, techniques for identifying and evaluating faults have been developed to enhance the dependability and availability of these systems [1]. Bearing malfunctions account for forty percent of motor failures [2], highlighting the significance of identifying issues with bearings for supervising the condition of rotary machines. Currently, there are multiple methods to monitor and diagnose motor bearing faults, such as analyzing of vibration signals [3], monitoring

acoustic signals [3], supervising electromagnetic fields [4], and analyzing the motor current signal (MCSA) [5]. Among these techniques, MCSA shows promise for diagnosing faults in induction motors. The need for additional sensors is eliminated by current signal-based monitoring, unlike traditional sensor-based monitoring methods that require accelerometers mounted on the tested motor for vibration-based monitoring. As a result, current-based motor fault monitoring systems have simpler designs and are easier to implement.

The crucial steps in diagnosing bearing failures using vibration or current data involve feature extraction and fault classification. Common techniques for feature extraction from the signals include Fast Fourier Transform (FFT) [6], Discrete Wavelet Transform (DWT) [6], Empirical Mode Decomposition (EMD) [7]. Several typical machine learning algorithms such as Support vector machines (SVM) [8], backpropagation (BP) neural networks [9], and k-Nearest Neighbor (k-NN) [10] are used for the bearing fault classification. Nonetheless, these methods demand significant expertise in feature extraction and data preprocessing. Additionally, selecting the optimal features from a dynamic environment poses a challenge. For example, extracted features may fail to effectively represent faults if the fault signal is exceedingly weak. Consequently, fault diagnosis would be challenging, especially given the variety of working environments [11].

One advantage of deep learning compared with traditional machine learning techniques, such as SVM, KNN, and RF lies in its ability to automatically extract features without human intervention and to classify data using nonlinear activation functions at each layer. Convolutional Neural Networks (CNN) represent a typical type of deep neural network with numerous advantages in facial recognition or image processing. In recent years, researchers have explored the application of CNNs in processing bearing fault signals. Hoang and Kang [12] delved into deep learning techniques alongside information fusion methodologies for the diagnosis of bearing faults. Their methodology involved utilizing samples from two phases of motor current signals as inputs for two distinct CNNs. Subsequently, they proposed a model combining a convolutional neural network with SVM, k-NN, and multi-layer perceptron architectures, culminating in a commendable maximum diagnostic accuracy of 98.30% under noise-free conditions. Wang et al. [13] applied wavelet-based filtering technique to denoise two-phase current signals before employing a CNN-SVM hybrid model for fault bearing diagnosis, resulting in an impressive accuracy rate of 99.01%. Ma et al. [14] from Foshan University, China, proposed a fault diagnosis method for motor bearings based on current Bi-Spectrum and CNN, obtaining a diagnostic accuracy of 80%.

Within the context of our survey, published studies on bearing fault diagnosis utilize CNN networks to examine motor current signals either in the time domain [12, 13], or frequency domain [14]. These both studies did not employed the combination of signals in time and frequency domains. When representing the motor current signal in the time domain, only the fault occurrence time is known, but it exhibits negligible variation [15]. Therefore, when affected by noise, it is difficult to accurately diagnose the bearing fault based on the features only in the time domain. In addition, according to [16], the bearing fault leads to significant changes in the stator current spectrum, and this spectrum can be used for fault diagnosis purposes. For this reason, signal analysis in both the time and frequency domains is necessary to enhance the accuracy of bearing fault diagnosis. It is necessary to design a 2-input CNN network with the signal as the time domain and the spectrum of the signal to simultaneously extract the features of the signal in both domains, or use two independent CNN networks, each used to extract the signal in one domain and then merge them to analyze the inter-domain signal [12]. Nevertheless, the fault classification accuracy when experimenting with the IF-CNN model in [12] using raw signals and their spectral portrait as inputs is lower than when experimenting with the model using pre-processed input data. However, because the author uses the output of the last layer of CNN to combine information from two CNNs, based on the information in this last layer, the model already knows the exact classification probability of the test data on each domain, so the essence is still extracting information from two independent domains. The problem of analyzing inter-domain signals has not been completely solved. Additionally, these studies have not explored how adding noise to signals with varying levels impacts diagnostic accuracy. Consequently, these methods are only applicable to laboratory data. In practical situations where fault signals are masked by background noise, existing methods might diminish their efficacy.

This work proposes a new solution for bearing fault diagnosis using an MI-CNN, which involves utilizing estimated current signals and their spectral portrait after FFT transformation. Initially, motor current signals are estimated employing a Kalman Filter. Subsequently, both the estimated current signals corresponding to various fault conditions of motor bearings and their FFT signals are simultaneously extracted using the proposed MI-CNN. In order to identify different types of bearing faults, the extracted features are combined through a combined block during the fusion stage and then classified via a softmax classifier. The experiments are carried out on both types of noise-free signals and the signals with added noise at varying levels. Furthermore, the parameters of the proposed MI-CNN model are optimized to improve the accuracy of the

proposed method based on the test results of fault classification accuracy for different values of model parameters. Moreover, experiment results are compared with existing techniques on the same datasets to demonstrate the robustness of the proposed method.

This work provides the main contributions as follows:

- Proposing a novel approach that enhances fault diagnosis efficiency by integrating both estimated motor current signals and their FFT counterparts with deep learning techniques.

- Employing a MI-CNN architecture to compare the effectiveness of the proposed method against published approaches.

- Validating the effectiveness of the proposed method through a series of experiments involving both noise-added and noise-free signals.

The remainder of this paper is organized as follows. Section 2 presents the proposed algorithm for the motor bearing fault diagnosis. In Section 3, the experiment dataset and method will be discussed in detail. Then, Section 4 provides the results and discussions of the proposed algorithm. Finally, Section 5 concludes the paper.

2. Proposed method

Fig. 1 demonstrates the proposed method to diagnose bearing failures. According to Fig. 1, the depicted approach encompasses four main phases: data collection, feature extraction, fusion phase, and classification phases. Within the data collection phase, two principal tasks are undertaken: estimating current signals from the dataset, referred to as signals in the time domain, and conducting FFT on the estimated signals, termed signals in the frequency domain. These signals are then structured as grayscale images and inputted into the innovative CNN. Feature extraction is concurrently performed on both the time domain and frequency domain signals using 5 CNRM blocks along with a pair of Fully Connected and ReLU layers. All features are extracted from the estimated current signal and their FFTs are fed into the feature fusion stage to improve fault classification reliability. In the classification phase, a softmax layer receives the fused features and employs them to categorize the bearing-fault signals. The detailed parameters in each layer are listed in Table 12. Subsections 2.1 to 2.3 will detail the steps in the proposed method.
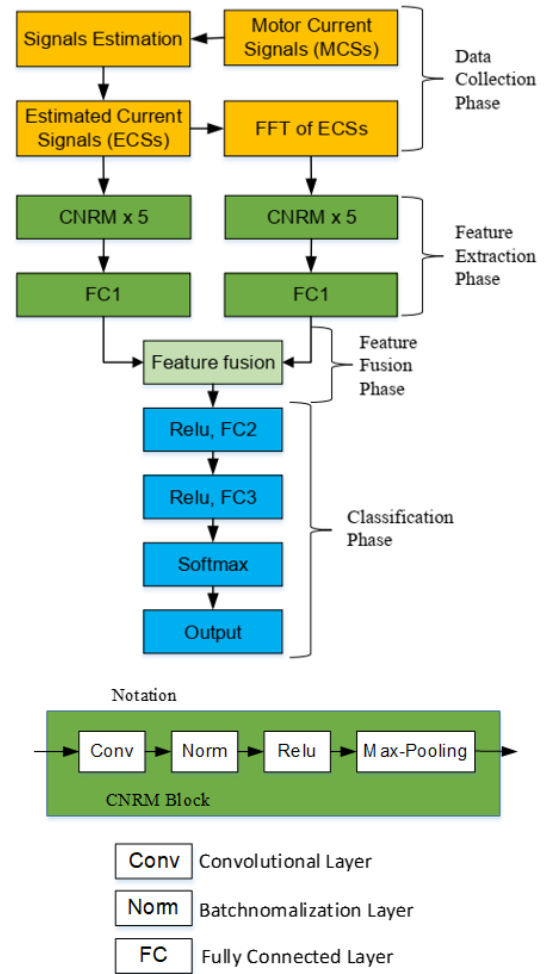

Fig. 1: Overall diagram of proposed approach for bearing fault detection.

2.1. Motor current signal estimation based on Kalman filter

The state space equation of the system in signal space is defined as follows:

$$\mathbf{x}_{n+1} = \mathbf{F}_n\mathbf{x}_n + \mathbf{w}_n, \quad \mathbf{z}_n = \mathbf{H}_n\mathbf{x}_n + \mathbf{v}_n \qquad (1)$$

where $\mathbf{F}_n$ is the status transformation matrix, its size is $(n_x \times n_x)$; $\mathbf{H}_n$ is the measuring matrix, its size is $(n_z \times n_x)$; n is the discrete-time index; $\mathbf{x}_n$ represents the status vector of bearings, its size is $(n_x \times 1)$, which means $\mathbf{x}_n$ is a vector containing elements of 0, 1, or 2 if the bearing has no fault, outer race faults, or inner race faults, respectively; the supervision vector is denoted by $\mathbf{z}_n$, comprises chosen current signals from the dataset, with a size of $(n_z \times 1)$; $\mathbf{w}_n$ is process interference vector, its size is $(n_x \times 1)$; $\mathbf{v}_n$ is measuring interference vector, its size is $(n_z \times 1)$.
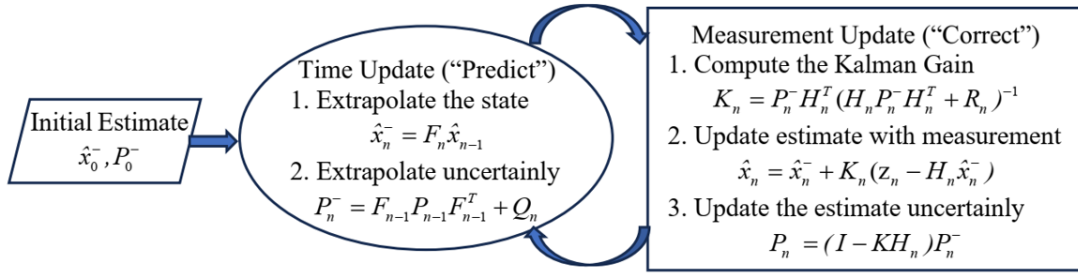
Fig. 2: The stages of current signal estimation based on Kalman filter (I is the unit matrix).

Equations (2) and (3) provide the covariance matrices of the $\mathbf{w}_n$ and $\mathbf{v}_n$ vectors.

$$E\left[\mathbf{w}_n \mathbf{w}_i^T\right] = \begin{cases} \mathbf{Q}_n, & i = n \\ \mathbf{0}, & i \neq n \end{cases} \tag{2}$$

$$E\left[\mathbf{v}_n \mathbf{v}_i^T\right] = \begin{cases} \mathbf{R}_n, & i = n \\ \mathbf{0}, & i \neq n \end{cases}, \quad E\left[\mathbf{w}_n \mathbf{v}_i^T\right] = \mathbf{0} \quad \forall n, i \tag{3}$$

where T denotes the matrix transpose, $E[.]$ denotes the expectation function, $\mathbf{Q}_n$ is the process noise covariance, $\mathbf{R}_n$ is the measurement noise covariance. Measuring interference $\mathbf{v}_n$ can include intrinsic interference sources such as defects in the manufacture and installation of bearings, roller, and drive shaft. In reality, the noise sources do not reflect the occurrence of bearing failures. Consequently, $\mathbf{v}_n$ in Eq. (1) mainly describes the internal noise sources, which exist only during the operation of the rotating machinery.

Next, a linear Kalman filter [17, 18] is utilized for the system model in Eq. (1) for status estimation. The condition estimate graph is depicted in Fig. 2. Kalman gain K is calculated as the first step in processing an estimate utilizing the $\mathbf{R}_n$ and the related error covariance $\mathbf{P}_n^-$ provided by Eq. (4).

$$\mathbf{P}_n^- = E\left[\mathbf{e}_n^- \mathbf{e}_n^{-T}\right], \quad \bar{\mathbf{e}}_n = \mathbf{x}_n - \widehat{\mathbf{x}}_n^- \tag{4}$$

Where, $\widehat{\mathbf{x}}_n^-$ shows the predicted state, $\mathbf{e}_n^-$ shows the prediction error. Next, the status assessment $\widehat{\mathbf{x}}_n$ is updated by using the Kalman gain $\mathbf{K}$ and the observation $\mathbf{z}_n$; then we can calculate the error covariance $\widehat{\mathbf{P}}_n$ defined as follows:

$$\mathbf{P}_n = E\left[\mathbf{e}_n \mathbf{e}_n^T\right], \quad \mathbf{e}_n = \mathbf{x}_n - \hat{\mathbf{x}}_n \tag{5}$$

Where, $\mathbf{e}_n$ is the error of the assessment.

The stages of current signal estimation based on the Kalman filter as shown in Fig. 2 can be described as follows: Firstly, an estimation of x_{n-1} (indicated $\widehat{x}_{n-1}$) and the covariance of that estimation (indicated p_{n-1}) for current signal at time n-1 are determined. Subsequently, an estimation of x_n (indicated $\widehat{x}_n^-$) and the covariance of that prediction (indicated P_n^-) at time n

are calculated based on $\widehat{x}_{n-1}$ and p_{n-1}. Then sample update is implemented at time n to correct its prediction of x_n. The resulting estimation of x_n is signified $\widehat{x}_n$ and the covariance of that estimation is signified P_n. Initializing the values $\hat{\mathbf{x}}_0^-, \mathbf{P}_0^-$ is fundamental step of the status assessment process. These values could be defined by Eq. (6):

$$\widehat{\mathbf{x}}_0^- \approx \widehat{z} = \frac{1}{\mathbf{N}} \sum_{j=N}^{-1} z_j;$$

$$\mathbf{P}_0^- = E[e_0^- e_0^{-T}] = \mathbf{R}_0 \approx \frac{1}{\mathbf{N}} \sum_{j=N}^{-1} (z_j - \bar{z})(z_j - \bar{z})^T \tag{6}$$

Where $\mathbf{z}_j's, \quad j = -N, -N+1, \ldots, -1$ are N previous measurements and $\mathbf{e}_0^- = \mathbf{x}_0 - \widehat{\mathbf{x}}_0^-$ is the initial assessment error and $\mathbf{R}_0$ is its covariance matrix.

This estimation is performed frame by frame for all data points that are the results of the motor current signal measurements corresponding to the different bearing states and the estimation process reiterates with the whole input data. Subsequently, the estimated motor current signal is transformed from the time domain to the frequency domain using the FFT technique.

2.2. Fast Fourier Transform of the estimated motor current signal

The purpose of transforming the estimated signal into the frequency domain before inputting it into the CNN network is to enable the CNN to discern features across both time and frequency domains, unlike prior methods that focused solely on either the time or frequency domain [12, 13] and [14].

2.3. Construct the proposed MI-CNN for bearing fault diagnosis

A normal CNN includes the input layer, convolutional layer, pooling layer, fully connected layer, and output

layer. More details about Convolutional Neural Networks can be found in [19]. Applying the fundamental concepts of the basic CNN, in this work, a modified structure CNN, called MI-CNN for fault diagnosis in bearings using motor current signals is proposed with the details as follows.

The data collection and feature extraction stages consist of two branches: the left and right branches, which are used to collect and extract features using signals from ECSs and their FFT, respectively. Two branches have an identical structure. Data points from ECSs and their FFT are first converted into gray images of dimensions L1 x L2. These images are fed to the two inputs of the MI-CNN network, each branch of this network comprises five CNRM blocks and a fully connected block (FC1). The first four CNRM blocks share the same structure consisting of a convolutional layer, a normalization layer, a nonlinear activation layer, and a pooling layer. The fifth CNRM block includes a convolutional layer, a normalization layer, and a nonlinear activation layer. Padding is applied at the convolutional layers, with a stride of 1 x 1 after each multiplication, ensuring that no information is lost and that the image dimensions remain unchanged. The output from the first fully connected layer (FC1) is then fed into the feature fusion block, where extracted features from ECSs and their FFT of the current signals are combined, allowing the improved CNN network to further refine the feature extraction process. The number of neurons in the feature fusion block corresponds to the combined neurons of FC1 of each branch. As a result, the proposed MI-CNN network is capable of simultaneously extracting features from both the time and frequency domains of the current signal.

The feature classification stage consists of two pairs of ReLU and fully connected layers, followed by a Softmax layer and an output layer. The FC2 layer in the MI-CNN network contains 200 neurons, followed by the second fully connected layer (FC3) with 100 neurons and the output layer with 3 neurons. These neurons correspond to the bearing condition labels: 0, 1 and 2, representing a healthy bearing, a bearing with inner ring damage and a bearing with outer ring damage, respectively. This stage classifies the input image into one of three categories, labeled 0, 1 or 2, corresponding to different bearing fault conditions, based on the probabilities calculated by the Softmax layer. Subsequently, experiments are conducted on datasets outlined in Subsection 3.1 with different values of model parameters such as the number and the size of input data samples, the number and the size of kernel to suggest the optimal parameters of the proposed CNN. Finally, the accuracy of the proposed CNN is compared with that of other methods on identical datasets to validate the effectiveness of the proposed approach.

The next section of the paper will present the dataset for experimental verification of the suggested MI-CNN effectiveness, the scenario and experimental method.

3. Experiments

3.1. Experimental dataset

In order to validate the accuracy of proposed solution for bearing fault diagnosis, we utilize the dataset which is provided by Paderborn University [20]. This is a laboratory-measured dataset and has been used by many research groups to test the proposed bearing fault diagnosis solution ([12, 13, 14], and [15]). This dataset comprises 20 measurements over 4 seconds of various motor parameters such as the radial force (F), the torque (M), the speed (S), the vibration signal, the oil temperature of the bearing module, the phase-1 of the current signal (PH1), and the phase-2 of the current signal (PH2) across 32 different bearing codes of type 6203, encompassing 6 codes for healthy bearings (K001-K006), 12 for outer-race-faulty bearings (KA01, KA03-KA09, KA15, KA16, KA22, KA30), 11 for inner-race-faulty bearings (KI01, KI03-KI05, KI07, KI08, KI14, KI16-KI18, KI21), and 3 for bearings with both inner-race and outer-race faults (KB23, KB24, KB27). The motor (1) is a 425 W permanent magnet synchronous motor (PMSM) with a rated torque of T = 1.35 Nm, a rated rotor shaft speed of n = 3000 rpm, a rated current of I = 2.3 A and the number of pole pairs of p = 4. It is operated by a frequency converter (KEB Combivert 07F5E 1D-2B0A) with a cut-off frequency of 16 kHz. This motor has 4 working conditions corresponding to different values of rotor shaft rotation speed (S), load torque (M), radial force acting on bearings (F). In this article, we utilized the PH1 of fifteen bearing codes in Table 1 with working condition B of the motor in Table 2 to do experiment.

3.2. Experimental method

The data points of phase-1 of the motor current signals with labels K0, KA and KI in Table 2 are arranged into data frames of L1 x L2 size. Each of these frames corresponds to an image of size L1 x L2 pixels. Therefore, the number of images corresponding to the labels K0, KA, and KI in Table 1 is 25.600.000/(L1 x L2) images. The allocation of input images to the MI-CNN network is performed randomly as follows: 80% of the images are assigned for training and the remaining 20% are reserved for testing and evaluation. The parameters of the MI-CNN network for the experiment are listed in Table 3.

Tab. 1: Bearing codes for effectiveness verification.

Condition of bearings	Class	Label	Bearing codes for experiment	Number of measurements/ bearing code	Duration for a measurement	Sampling frequency
No fault (N)	0	KO	01, 02, 03, 04, 05	20	4 seconds	64 kHz
Outer-race fault (O)	1	KA	04, 15, 16, 22, 30	20	4 seconds	64 kHz
Inner-race fault (I)	2	KI	04, 14, 16, 18, 21	20	4 seconds	64 kHz

Tab. 2: Engine working conditions.

Working condition	S (RPM)	M (Nm)	F (N)
A	1500	0.1	1000
B	900	0.7	1000
C	1500	0.7	400
D	1500	0.7	1000

Tab. 3: Parameters of the proposed MI-CNN.

Parameter	Value
Input image size	L1 $\times$ L2
Minibatch Size	128
InitialLearnRate	α
LearnRateDropFactor	0.1
ValidationPatience	5
L2Regularization	1e-10
Epoch	10
The number of kernels/the kernel size per convolutional layers	K/F
Optimizer	Adam

The mini-batch size is chosen to be 128. If the value of the mini-batch size is too small, the number of iterations will increase, leading to the state of the model gradually moving from underfitting to optimal and then overfitting. On the contrary, if the mini-batch size is too large, more buffers memory is needed to store the training data. Furthermore, to verify the effectiveness and reliability of the model, Gaussian noise was added to the signals used for testing. In this study, the proposed method is tested by changing the coefficients L1, L2, α, K, F on signals with different signal-to-noise ratios from -10 dB to 20 dB with a step of 5 dB to select the optimal parameter set for the model. The selection is based on the criteria of fault classification accuracy and execution time. It is worth noting that the purpose of selecting the optimal parameter set during the fine-tuning phase is to establish a configuration that ensures fast execution time while enhancing fault classification accuracy for real-time applications. After selecting the optimal parameter set, we compare the electric motor bearing fault classification accuracy of the proposed so-lution using the proposed MI-CNN model with several different methods implemented using the current signal and CNN including a deep learning and information fusion method [12], combined method using wavelet filter, CNN and SVM [13], the Bi-Spectrum method [14] using the same dataset, executed on the same hardware platform (Intel (R) Core i7 2.9 GHz CPU; 8 GB RAM) using MATLAB software to highlight the effectiveness of the proposed method.

4. Results and discussion

4.1. The accuracy of bearing fault diagnosis across varied initial Learning Rate

In this experiment, we selected the proposed MI-CNN model with a random set of values: L1 x L2 (80 x 80), K (5), F (3 x 3) and varied the learning rate (0.001, 0.01, and 0.1). The dataset used for the experiment corresponds to working condition B in Table 2. The value of the learning rate will directly affect the convergence speed of the loss function to the global extreme point.

Fig. 3 and Table 4 show the classification accuracy of motor bearing faults of proposed CNN model with different initial learning rate. According to Fig. 3, with a large initial learning rate for example 0.1, the classification accuracy is low, especially for signals with small SNR. Whereas a high classification accuracy is achieved even with signals with small value of SNR (such as -10 dB), if we use small initial learning rates such as 0.01 or 0.001.

To mitigate the overfitting problem, we applied L2 regularization during training with a penalty factor of 0.00001. Additionally, we augmented the dataset by adding noise with signal-to-noise ratios (SNR) ranging from -10 dB to 20 dB. This approach increased the dataset's diversity and further reduced overfitting. As shown in Fig. 4, the validation loss and validation accuracy closely align with the training loss and training accuracy, indicating that overfitting has been significantly reduced.

Tab. 4: Fault classification accuracy with different initial learning rates.

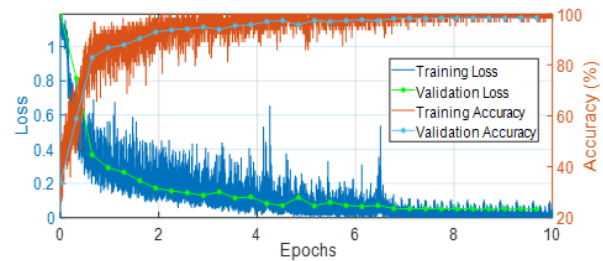| The initial learning rates	The fault classification accuracy (%) with the noise-adding signal at the different SNR						
	20 dB	15 dB	10 dB	5 dB	0 dB	-5 dB	-10 dB
0.1	76.67	75.17	72.62	63.21	53.25	40.79	38.96
0.01	98.62	98.45	98.12	97.82	97.56	97.00	96.12
0.001	99.76	99.73	99.71	99.58	99.54	99.46	99.14

Tab. 5: Fault classification accuracy with varying input image sizes.

Input image size	Fault classification accuracy (%) with noise-adding signal at different SNR values						
	20 dB	15 dB	10 dB	5 dB	0 dB	-5 dB	-10 dB
40 × 40	98.55	98.35	98.34	96.16	95.13	91.28	88.55
60 × 60	92.43	83.47	83.24	68.70	67.10	66.10	65.82
80 × 80	99.76	99.73	99.71	99.58	99.54	99.46	99.14
100 × 100	99.28	93.31	90.80	86.54	85.14	81.96	76.95
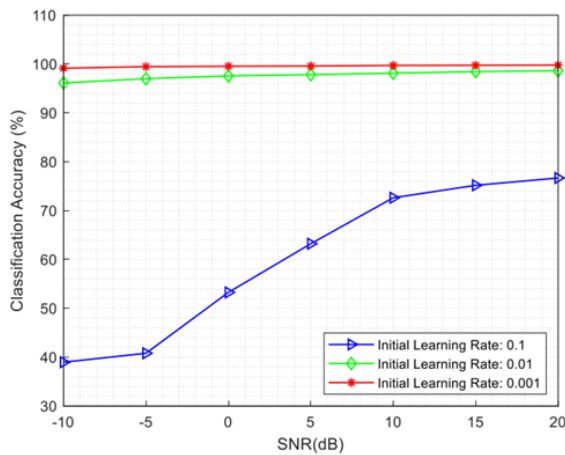
Fig. 3: Performance of proposed CNN model with different initial learning rate.

Fig. 4: Loss and accuracy in training process of the MI-CNN model with initial learning rate $\alpha = 0.001$.

4.2. The accuracy of bearing fault diagnosis across varied size of input data image

In this part, we selected the MI-CNN model with F = 3 x 3, K = 5, $\alpha = 0.001$ and varying the L1 x L2 values of 40 x 40, 60 x 60, 80 x 80, and 100 x 100 to evaluate the classification accuracy. The mini-batch size and the epoch are chosen as in Table 3. The dataset used for the experiment corresponds to working condition B in Table 2. The fault classification accuracy curves corresponding to different input data image sizes are shown in Fig. 5. The fault classification accuracy and the classification time for one image and the number of learnable parameters of this CNN model with different input data image sizes are depicted in Table 5 and Table 6, respectively. From Fig. 5, it can be seen that input images sized at 40 x 40, 60 x 60, or 100 x 100 exhibit lower classification accuracy compared with those

with dimensions 80 x 80. This is because the process of estimating and extracting the spectrum of the motor current signal is performed on frames of 6400 data points. Therefore, when arranging these frames into images of size 80 x 80 (6400 data points) to input into the MI-CNN model, there is no residual, meaning the fault information is fully contained in a single input image. However, when using input images with sizes of 40 x 40 (1600 data points), 60 x 60 (3600 data points), or 100 x 100 (10000 data points), arranging the frames of 6400 data points into these images results in the fault information being spread across multiple images.

According to Table 5, it is clear that a larger number of learnable parameters results in longer classification times for data images. Fig. 5 and Table 6 reveal that the model utilizing 40 x 40 input data images exhibit a relatively short prediction time (1.090 ms ± 10%), and its classification accuracy is inferior to that of the model employing 80 x 80 input data image. Conversely, the model utilizing 100 x 100 input data images not only demonstrate reduced classification accuracy (particularly for signals with low SNRs) but also incurs a longer execution time (5.814 ms ± 10%) compared with other input data image sizes. Although the model employing 60 x 60 input data images yield a shorter

Tab. 6: Time for prediction a data image, the number of learnable parameters for the proposed model with different sizes of input data image.

Size of input image	Number of data images need to specify	Time for prediction a data image (ms)	The number of learnable parameters
40×40	9600	$1.090 \pm 10\%$	50843
60×60	4267	$2.035 \pm 10\%$	60843
80×80	2400	$3.430 \pm 10\%$	92843
100×100	1536	$5.814 \pm 10\%$	114843
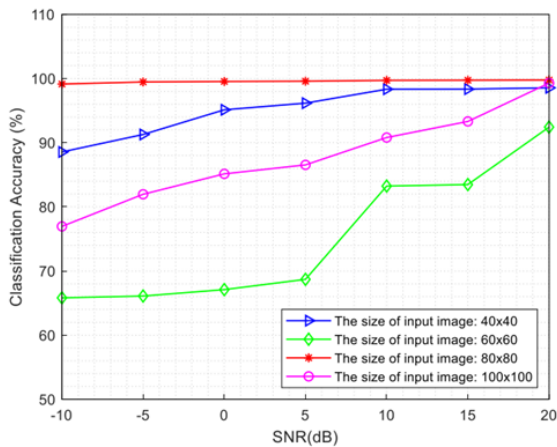
Fig. 5: Classification accuracy curves of proposed algorithm with different size of input data image.
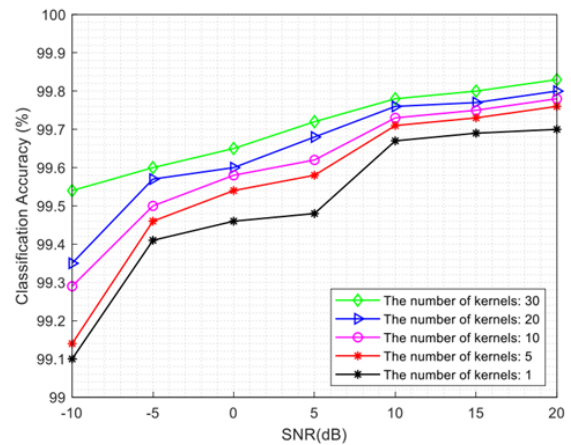
Fig. 6: Classification accuracy curves of proposed algorithm with different number of kernels.

prediction time than the one with 80 x 80 input data images (2.034 ms $\pm$ 10% compared with 3.430 ms $\pm$ 10%), the former achieves lower classification accuracy than the latter. Based on the aforementioned analysis, a model with an input data image size of 80 x 80 is chosen to strike a balance between failure classification accuracy and execution time.

4.3. The accuracy of bearing fault diagnosis across varied number of kernels

In this experiment, we selected the proposed MI-CNN model with a random set of values: L1 x L2 (80 x 80), F (5 x 5), α(0.001) and varied the K values of 1, 5, 10, 20, and 30. The dataset used for the experiment corresponds to working condition B in Table 2 with added Gaussian noise at different SNR values. Fig. 6 illustrates the classification accuracy of motor bearing faults for five different kernel quantities per convolutional layer using the proposed MI-CNN model. The results of bearing fault classification accuracy, the time taken to classify a single image and the number of learnable parameters of the proposed model with varying kernel quantities are presented in Tables 7 and 8, respectively.

On one hand, increasing the number of kernels in each convolution layer tends to enhance classification accuracy by enabling the network to deeply learn signal features. For signals with large SNR (such as 10, 15, 20 dB), adjusting the kernel number has negligible impact on classification accuracy. Conversely, for signals with low SNR (such as -10 dB), there is a slight effect on accuracy, shifting from 99.10% with one kernel to 99.54% with thirty kernels. On the other hand, augmenting kernel numbers substantially escalates the total learnable parameters of the CNN model, soaring from 50923 with one kernel to 407043 with thirty kernels. As a result, the prediction time for image data of CNN models also increases from 3.339 ms $\pm$ 10% to 6.336 ms $\pm$ 10%. This analysis suggests that while increasing filter numbers in the proposed CNN model does not significantly bolster fault classification accuracy, it markedly elongates execution time. Therefore, for the CNN model in this study, a kernel number of 5 is chosen to strike a balance between accuracy and real-time responsiveness.

4.4. The accuracy of bearing fault diagnosis across varied size of kernels

In this experiment, we utilize L1 x L2 (80 x 80), K (5), α (0.001), the mini-batch size and the epoch are

Tab. 7: Fault classification accuracy with varying numbers of kernels.

Number of kernels	Fault classification accuracy (%) with the noise-adding signal at the different SNR						
	20 dB	15 dB	10 dB	5 dB	0 dB	-5 dB	-10 dB
1	99.70	99.69	99.67	99.48	99.46	99.41	99.10
5	99.76	99.73	99.71	99.58	99.54	99.46	99.14
10	99.78	99.75	99.73	99.62	99.58	99.50	99.29
20	99.80	99.77	99.76	99.68	99.60	99.57	99.35
30	99.83	99.80	99.78	99.72	99.65	99.60	99.54

Tab. 8: Time for prediction a data image, the number of learnable parameters for the proposed model with different number of kernels.

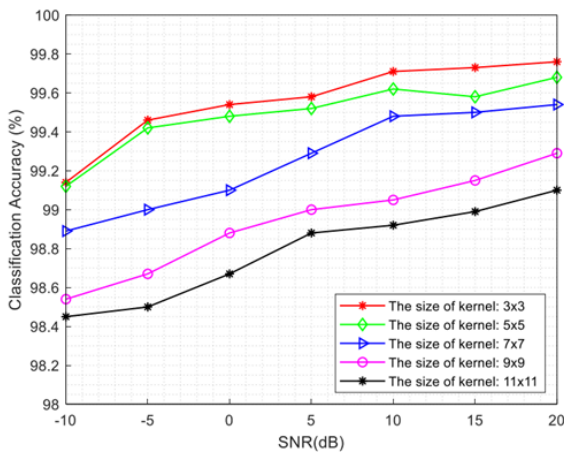| Number of kernels	Number of data images need to specify	Time for prediction a data image (ms)	The number of learnable parameters
1	2400	$3.339 \pm 10\%$	50923
5	2400	$3.430 \pm 10\%$	92843
10	2400	$4.163 \pm 10\%$	148483
20	2400	$5.265 \pm 10\%$	270563
30	2400	$6.336 \pm 10\%$	407043

Fig. 7: Classification accuracy curves of proposed algorithm with different kernel sizes.
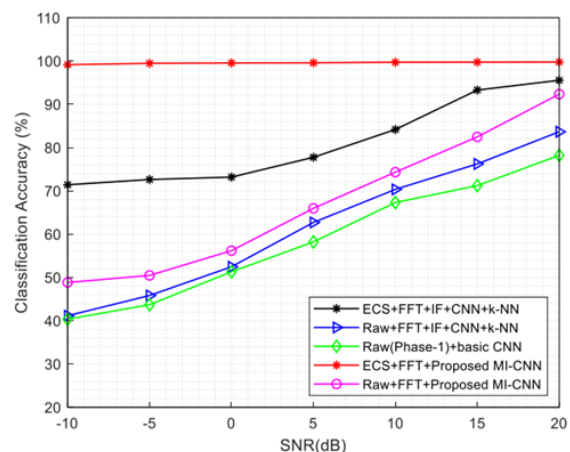

Fig. 8: Fault classification accuracy comparison of the proposed MI-CNN model with IF+CNN+k-NN for noise-added signals.

selected as in Table 3. We change the size of kernels such as 3 x 3, 5 x 5, 7 x 7, 9 x 9, and 11 x 11 to evaluate the classification accuracy. The dataset used for the experiment corresponds to working condition B in Table 2 with added Gaussian noise at different SNR values. The fault classification accuracy curves corresponding to kernel sizes are shown in Fig. 7. The results of bearing fault classification accuracy and the classification time for one image, the number of learnable parameters of the proposed MI-CNN model with different kernel sizes are depicted in Tables 9 and 10, respectively.

Fig. 7 and Table 10 indicate that in the proposed CNN model across signals with varying SNRs, enlarging the filter size not only reduces fault classification accuracy but also marginally prolongs execution time.

For instance, considering a signal with 10 dB SNR, as the filter size increases from 3 x 3 to 5 x 5, 7 x 7, 9 x 9, and 11 x 11, the fault classification accuracy decreases slightly from 99.71% to 99.62%, 99.48%, 99.05%, and 98.92%, respectively. Consequently, the filter size of the proposed model in this study is chosen to be 3 x 3 due to its higher accuracy and faster execution time compared to other kernel sizes.

The optimal parameter set and structure for the proposed MI-CNN model which are outlined in Table 11 and Table 12 are selected according to the experimental results from 4.1 to 4.4. With such a lightweight structure, our proposed model has the potential for deployment in resource-limited systems, such as Raspberry Pi or Jetson Nano.

Tab. 9: Fault classification accuracy with varying kernel sizes.

Kernel size/ convolutional layers	Fault classification accuracy (%) with noise-adding signal at different SNR values						
	20 dB	15 dB	10 dB	5 dB	0 dB	-5 dB	-10 dB
3×3	99.76	99.73	99.71	99.58	99.54	99.46	99.14
5×5	99.68	99.64	99.62	99.52	99.48	99.42	99.12
7×7	99.54	99.50	99.48	99.29	99.10	99.00	98.89
9×9	99.29	99.15	99.05	99.00	98.88	98.67	98.54
11×11	99.10	98.99	98.92	98.88	98.67	98.50	98.45

Tab. 10: Time for prediction a data image, the number of learnable parameters for the proposed model with different kernel sizes.

Kernel size	Number of data images need to specify	Time for prediction a data image (ms)	The number of learnable parameters
3×3	2400	$3.430 \pm 10\%$	92843
5×5	2400	$3.564 \pm 10\%$	96203
7×7	2400	$3.719 \pm 10\%$	101243
9×9	2400	$3.873 \pm 10\%$	107963
11×11	2400	$3.973 \pm 10\%$	116363

Tab. 11: Parameters of the proposed MI-CNN model.

Parameter	Value
Input image size (L1 $\times$ L2)	80×80
Minibatch size	128
InitialLearnRate	0.001
LearnRateDropFactor	0.1
LearnRateDropPeriod	20
ValidationPatience	5
L2Regularization	1e-10
Epoch	10
Number of kernels in convolutional layers	5
Kernel size in convolutional layers	3×3
Optimizer	Adam
Number of convolutional layers	5

4.5. Comparison of bearing fault classification accuracy the proposed MI-CNN model with other MI-CNN

In this experiment, we compare the classification accuracy of the proposed MI-CNN model with IF-CNN [12] when input data is raw signals and their spectral portrait. Then, we change the input data to be the estimated signals and their spectral portrait. The dataset used for the experiment corresponds to working condition B in Table 2 with added Gaussian noise. The classification accuracy of motor bearing faults of the proposed CNN model and IF+CNN+k-NN [12] are depicted in Table 13 and Fig. 8.

According to Table 13 and Table 14, bearing fault classification accuracy of both the proposed MI-CNN

model and the IF-CNN model with input data is both estimated motor current signals and their FFT is higher than that model with input data is both raw motor current signals and their FFT and the basic CNN model with raw motor current signal for all SNR values. However, applying the Kalman filter in the preprocessing stage introduces a slight delay (0.21 ms) compared to not using it. Despite the additional computational complexity, the Kalman filter enables the MI-CNN model to achieve significantly higher accuracy in bearing fault classification even though with low SNR signal (-10 dB, -5 dB, and 0 dB). Therefore, the use of the Kalman filter offers a favorable trade-off between classification accuracy and computational complexity. The basic CNN performs bearing fault classification based on raw motor current signals, allowing it to execute faster than the MI-CNN and IF+CNN models. However, it provides significantly lower classification accuracy. Despite obtaining the high classification accuracy, employing Kalman filter and FFT for preprocessing combined with the prposed MI-CNN model makes the prediction time slower than IF-CNN model and basic CNN model as shown in Table 14.

4.6. Evaluating the performance of the proposed CNN model against other studies

In this experiment, several different methods, including the information fusion method [12], wavelet CNN-SVM [13], and current Bi-Spectrum and CNN [14], were implemented alongside the suggested solution with the same dataset to evaluate the effectiveness of the recommended solution. The dataset of bearing-fault samples used for performance comparison consists of original

Tab. 12: Structure of the proposed MI-CNN model.

Layer	Block	Kernel size/number	Input Size	Output Size
CL1	CNRM 1	$3 \times 3/5$	80×80	80×80
PL1	CNRM 1	$2 \times 2/5$	80×80	40×40
CL2	CNRM 2	$3 \times 3/5$	40×40	40×40
PL2	CNRM 2	$2 \times 2/5$	40×40	20×20
CL3	CNRM 3	$3 \times 3/5$	20×20	20×20
PL3	CNRM 3	$2 \times 2/5$	20×20	10×10
CL4	CNRM 4	$3 \times 3/5$	10×10	10×10
PL4	CNRM 4	$2 \times 2/5$	10×10	5×5
CL5	CNRM 5	$3 \times 3/5$	5×5	5×5
CL6	CNRM 6	$3 \times 3/5$	80×80	80×80
PL6	CNRM 6	$2 \times 2/5$	80×80	40×40
CL7	CNRM 7	$3 \times 3/5$	40×40	40×40
PL7	CNRM 7	$2 \times 2/5$	40×40	20×20
CL8	CNRM 8	$3 \times 3/5$	20×20	20×20
PL8	CNRM 8	$2 \times 2/5$	20×20	10×10
CL9	CNRM 9	$3 \times 3/5$	10×10	10×10
PL9	CNRM 9	$2 \times 2/5$	10×10	5×5
CL10	CNRM 10	$3 \times 3/5$	5×5	5×5
FC1		5×5	5×5	200
FC2		400	400	100
FC3		100	100	3

Tab. 13: Comparison of bearing fault classification accuracy of proposed CNN model and IF-CNN model.

Method	Fault classification accuracy (%) with noise-adding signal at different SNR values						
	20 dB	15 dB	10 dB	5 dB	0 dB	-5 dB	-10 dB
Input Data: Raw motor current signals and their FFT							
Proposed MI-CNN	92.34	82.46	74.32	65.96	56.18	50.47	48.83
IF+CNN [12]	83.65	76.22	70.34	62.70	52.46	45.82	41.15
Input Data: Estimated motor current signals and their FFT							
Proposed MI-CNN	99.76	99.73	99.71	99.58	99.54	99.46	99.14
IF+CNN [12]	95.54	93.28	84.17	77.75	73.18	72.62	71.40
Input Data: Raw motor current signals (Phase-1)							
Basic CNN	78.20	71.20	67.30	58.20	51.30	43.70	40.35

data from Table 1, with noise-added signals at seven different SNR values of 20 dB, 15 dB, 10 dB, 5 dB, 0 dB, -5 dB, -10 dB. The fault classification accuracy curves corresponding to different methods with noise-added signals are depicted in Fig. 9. Table 15 presents the accuracy of various algorithms with both noise-free signals and noise-added signals. From Fig. 9 and Table 15, it is observed that with noise-free signal, the fault classification accuracy of the proposed method is 99.88%, which is only slightly higher than that of the wavelet CNN and SVM method, which achieves an accuracy of 99.32%.

In scenarios involving noise-added signals, the accuracy of all methods in Table 15 decreases as the SNR decreases. However, the accuracy of the proposed CNN model does not decrease significantly even for signals with low SNR. In contrast, the accuracy of other meth-

ods remains high only when the experiment's signals have high SNR values (10 to 15 dB). For low SNR signals (-10 to 0 dB), the accuracy of the published methods falls short of requirements due to ineffective preprocessing techniques in noisy environments. Among the methods listed in Table 15, apart from our proposed method with high accuracy, the classification accuracy of method [13] surpasses that of the remaining methods because it employs soft and hard threshold wavelet filters with fixed thresholds to eliminate the noise. However, this method has a limitation: when a small threshold level is utilized, removal is effective only for signals with high SNR (10 to 20 dB), resulting in classification accuracy exceeding 80%. Conversely, for signals with low SNR (-10 dB to 5 dB), the classification accuracy of this method is low because a small threshold level fails to filter out noise, while a

Tab. 14: Performance comparison of the proposed CNN model and IF-CNN model in terms of time for prediction a data image and the number of learnable parameters.

Method	Preprocessing time (ms)		Time for prediction a data image (ms)	The number of learnable parameters
	Kalman filter	FFT		
Input Data: Raw motor current signals and their FFT				
MI-CNN	0	0.15	$3.430 \pm 10\%$	92843
IF+CNN [12]	0	0.15	$1.501 \pm 10\%$	23296
Input Data: Estimated motor current signals and their FFT				
MI-CNN	0.21	0.15	$3.430 \pm 10\%$	92843
IF+CNN [12]	0.21	0.15	$1.501 \pm 10\%$	23296
Input Data: Raw motor current signals (Phase-1)				
Basic CNN	0	0	$1.120 \pm 10\%$	26223

Tab. 15: Comparison of the fault classification accuracy (%) of the proposed method and other methods with working condition B.

Solution	Noise-free signal	Fault classification accuracy (%) with noise-added signal at different SNR values						
		20 dB	15 dB	10 dB	5 dB	0 dB	-5 dB	-10 dB
ECS + FFT + Proposed MI-CNN (This paper)	99.88	99.76	99.73	99.71	99.58	99.54	99.46	99.14
Raw signal + IF+CNN +k-NN [12]	96.13	82.90	77.22	72.03	64.00	52.02	48.62	46.48
Raw signal + IF +CNN+ SVM [12]	96.13	83.50	77.40	75.50	66.02	56.10	52.70	48.30
Raw signal (Phase-1) + basic CNN	91.02	78.20	71.20	67.30	58.20	51.30	43.70	40.35
Wavelet + CNN + SVM [13]	99.32	93.70	85.88	80.33	72.12	62.36	56.72	50.22
Bi-Spectrum + CNN [14]	82.12	79.00	74.86	69.48	62.20	52.60	45.17	41.60

large threshold level causes loss of useful fault information. Thus, although it effectively removes noise, it results in the information loss. Due to the absence of noise elimination techniques in the information fusion method [12] and Bi-Spectrum and CNN methods [14], the classification accuracy is not notably higher than that of CNN model with raw signals. By utilizing the Kalman filtering algorithm to eliminate noise in the signal preprocessing stage and constructing an enhanced CNN model to learn signal features in both time and frequency domains during the feature extraction stage, the proposed method achieves nearly perfect accuracy (99.88%) with noise-free signals and approximately 99% accuracy with noise-added signals. Despite achieving very high classification accuracy, applying the trained model in practical applications faces significant challenges due to variations in real operational environments. Therefore, transfer learning should be used to retrain the pretrained model before deploying it in real applications.

5. Conclusion

The MI-CNN model based on the estimated motor current signals and their spectral portrait was used in this paper to present a novel bearing fault diagnosis technique. The proposed method incorporates the Kalman filtering algorithm to estimate the true status of motor current signals and eliminate associated noise. Subsequently, the ECSs are converted to frequency domain using the FFT technique. These ECSs and their FFT signals are then inputted into the proposed CNN model, enabling feature extraction from MCSs in both the time and frequency domains. Consequently, the classification accuracy is significantly enhanced, even for signals with low SNR values. Experimental results demonstrate that the proposed method achieves outstanding accuracies in bearing fault diagnosis under varying SNRs, surpassing other algorithms that analyze signals solely in the time or frequency domain and then employ CNN or CNN models combined with SVM or k-NN for training and classification. In addition, the parameters of the proposed CNN model are optimally selected through numerous experiments to evaluate fault classification accuracy when modifying
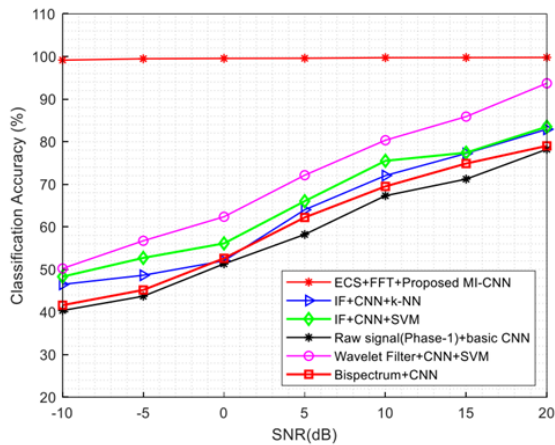
Fig. 9: Fault classification accuracy comparison of the proposed method with the other methods in case of noise-added signals.

parameters such as initial learning rate, number and size of kernels in each convolution layer, and length of input data image. In our future research, we will test the proposed algorithm using transfer learning on a broader range of motors and bearings under diverse working conditions.

Author Contributions

H.H.D. conducted experiments and wrote the whole paper. V.P.H. developed the system model. Both Q.T.B. and V.S.D. performed calculations related to signal estimation. All authors contributed to the final version of the manuscript. N.M.B. supervised the project.

Acknowledgment

References

[1] LIANG, X., M. Z. ALI, H. ZHANG. Induction Motors Fault Diagnosis Using Finite Element Method: A Review. *IEEE Transactions on Industry Applications.* 2020, vol. 56, no. 2, pp. 1205-1217. DOI: 10.1109/TIA.2019.2958908.

[2] HAKIM, M., A. A. B. OMRAN, A. N. AHMED, M. Al-WAILY, A. ABDELLATIF. A systematic review of rolling bearing fault diagnoses based on deep learning and transfer learning: Taxonomy, overview, application, open challenges, weaknesses and recommendations. *Ain Shams Engineering Journal.* 2023. vol. 14, iss. 4. DOI: 10.1016/j.asej.2022.101945.

[3] NIRWAN, N. W., H. B. RAMANI. Condition monitoring and fault detection in roller bearing used in rolling mill by acoustic emission and vibration analysis. *MaterialsToday: Proceedings.* 2022, vol. 51, pp. 344–354. DOI: 10.1016/j.asej.2022.101945.

[4] MINERVINI, M., M. E. MOGNASCHI, P. Di BARBA, L. FROSINI. Convolutional Neural Networks for Automated Rolling Bearing Diagnostics in Induction Motors Based on Electromagnetic Signals. *Applied Sciences.* 2021, vol. 11, no. 17. DOI: 10.3390/app11177878.

[5] DHOMAD, T. A., A. A. JABER. Bearing Fault Diagnosis Using Motor Current Signature Analysis and the Artificial Neural Network. *International Journal on Advanced Science, Engineering and Information Technology.* 2020, vol. 10, no. 1. DOI: 10.18517/ijaseit.10.1.10629.

[6] BESSOUS, N., S. SBAA, A. C. MEGHERBI. Mechanical fault detection in rotating electrical machines using MCSA-FFT and MCSA-DWT techniques. *Bulletin of the Polish Academy of Sciences. Technical Sciences.* 2019, vol. 67, no. 3. DOI: 10.24425/bpasts.2019.129655.

[7] GROVER, C., N. TURK. Rolling Element Bearing Fault Diagnosis using Empirical Mode Decomposition and Hjorth Parameters. *Procedia Computer Science.* 2020, vol. 167, pp. 1484–1494. DOI: 10.1016/j.procs.2020.03.359.

[8] HAN, T., L. ZHANG, Z. YIN, A. C. C. TAN. Rolling bearing fault diagnosis with combined convolutional neural networks and support vector machine. *Measurement.* 2021, vol. 177. DOI: 10.1016/j.measurement.2021.109022.

[9] LI, J., X. YAO, X. WANG, Q. YU, Y. ZHANG. Multiscale local features learning based on BP neural network for rolling bearing intelligent fault diagnosis. *Measurement.* 2020, vol. 153. DOI: 10.1016/j.measurement.2019.107419.

[10] WANG, H., Z. YU, L. GUO. Real-time Online Fault Diagnosis of Rolling Bearings Based on KNN Algorithm. *Journal of Physics: Conference Series.* 2020. DOI: 10.1088/1742-6596/1486/3/032019.

[11] LI, J., Z. YIN, F. ZHANG, G. XU, C. FAN, X. WANG. Bearing Fault Diagnosis Using

Residual Network and Attention Mechanism. *2022 IEEE 8th International Conference on Computer and Communications (ICCC), Chengdu, China.* 2022, pp. 132-138. DOI: 10.1109/ICCC56324.2022.10065917.

[12] HOANG, D. T., H. J. KANG. A Motor Current Signal-Based Bearing Fault Diagnosis Using Deep Learning and Information Fusion. *IEEE Transactions on Instrumentation and Measurement.* 2020, vol. 69, no. 6, pp. 3325-3333. DOI: 10.1109/TIM.2019.2933119.

[13] WANG, X., R. MENG, G. WANG, X. LIU, X. LIU, D. LU. The research on fault diagnosis of rolling bearing based on current signal CNN-SVM. *Measurement Science and Technology.* 2023, vol. 34, no. 12. DOI: 10.1088/1361-6501/acefed.

[14] MA, J., L. JIANG, S. LI, H. SHENG, C. ZHOU, X. LI. Fault diagnosis of motor bearing based on current Bi-spectrum and convolutional neural network. *Latin American Journal of Solids and Structures.* 2023, vol. 20, no. 5. DOI: 10.1590/1679-78257364.

[15] TOMA, R. N., J.-M. KIM. Bearing Fault Classification of Induction Motors Using Discrete Wavelet Transform and Ensemble Machine Learning Algorithms. *Applied Sciences.* 2020, vol. 10, no. 15. DOI: 10.3390/app10155251.

[16] BLODT, M., P. GRANJON, B. RAISON, G. ROSTAING. Models for Bearing Damage Detection in Induction Motors Using Stator Current Monitoring. *IEEE Transactions on Industrial Electronics.* 2008, vol. 55, no. 4, pp. 1813-1822. DOI: 10.1109/TIE.2008.917108.

[17] KAY, S. M. Fundamentals of statistical signal processing: Estimation theory. *Prentice-Hall, Inc..* 1993.

[18] BROWN, R. G., P. Y. HWANG. Introduction to random signals and applied Kalman filtering: with MATLAB exercises and solutions. 1997.

[19] ALZUBAIDI, L., et al. Review of deep learning: concepts, CNN architectures, challenges, applications, future directions. *Journal of Big Data.* 2021, vol. 8, no. 53. DOI: 10.1186/s40537-021-00444-8.

[20] LESSMEIER, C., J. K. KIMOTHO, D. ZIMMER, W. SEXTRO. Condition monitoring of bearing damage in electromechanical drive systems by using motor current signals of electric motors: A benchmark data set for data-driven classification. *PHM Society European Conference.* 2016, vol. 3, no. 1. DOI: 10.36001/phme.2016.v3i1.1577.